Contribution from the School of Chemistry, University of New South Wales, Kensington, N.S.W., 2033, and Department of Inorganic and Analytical Chemistry, La Trobe University, Bundoora, Victoria 3083, Australia

Triply Bridged Binuclear Thiolate Complexes of Oxomolybdenum(V). Synthesis of $[Mo_2O_2(SR)_6Z]^-$ (Z = OR′, SR′, NR′$_2$) and Crystal Structures of $(Et_4N)[Mo_2O_2(SCH_2CH_2O)_2Cl_3]$, $(Et_4N)[Mo_2O_2(SCH_2CH_2O)_3Cl]$, and $(Pr_3NH)[Mo_2O_2(SCH_2CH_2O)_3(SCH_2CH_2OH)]$

IAN W. BOYD,[1a] IAN G. DANCE,*[1b] ARTHUR E. LANDERS,[1b] and ANTHONY G. WEDD*[1a]

Received October 4, 1978

The reactions of various mononuclear oxomolybdenum(V) complexes with thiolate ligands have been studied and shown to produce triply bridged binuclear complexes. Three homologous diamagnetic complexes, $(Et_4N)[Mo_2O_2(SCH_2CH_2O)_2Cl_3]$, $(Et_4N)[Mo_2O_2(SCH_2CH_2O)_3Cl]$, and $(Pr_3NH)[Mo_2O_2(SCH_2CH_2O)_3(SCH_2CH_2OH)]$, have been isolated. Crystal structures determined for these three compounds reveal the common occurrence of a molecular structure containing a triply bridged pair of MoO units: the three monoanionic complexes differ in chloride/2-oxoethanethiolate substitution at nonbridging coordination sites. The triple bridge is formed by the sulfur (cis to both O=Mo bonds, mean Mo—S = 2.48 Å) and oxygen (approximately trans to both O=Mo bonds, mean Mo—O = 2.18 Å) atoms of one $^-SCH_2CH_2O^-$ ligand and the oxygen atom (cis to both O=Mo bonds, mean Mo—O = 2.03 Å) of a second $^-SCH_2CH_2O^-$ ligand which also chelates one molybdenum atom. Asymmetric six-coordination occurs for both molybdenum atoms. The binuclear complex is regarded as two square-pyramidal Mo=O units which share one edge of their basal coordination planes and also share one more weakly bound atom approximately trans to both Mo=O bonds. Mean Mo–Mo = 2.73 Å. The reaction between $MoOCl_3(THF)_2$ and alkylthiols in the presence of base in MeCN or DMF leads to the anions $[Mo_2O_2(SR)_7]^-$, of which the salts $B[Mo_2O_2(SR)_7]$ with quaternary cations have been isolated in substance. The mononuclear arylthiolato anions $[MoO(SAr)_4]^-$ (Ar = Ph, *p*-tolyl) react in the presence of a source of alkoxy or amido ligand, Z, to form related $B[Mo_2O_2(SAr)_6Z]$ salts. Such reactions are promoted by the oxidation of 1 mol of ^-SAr ligand by $FeCl_3$. Physical data indicate that these binuclear monoanions are also triply bridged species containing thiolate and Z bridging ligands. Structural and chemical implications of the stereochemistry of the triple bridge are discussed. Crystal data: $(Et_4N)[Mo_2O_2(SCH_2CH_2O)_2Cl_3]$, a = 12.877 (1) Å, b = 15.351 (1) Å, c = 13.147 (1) Å, β = 122.76 (1)°, $P2_1/c$, Z = 4; $(Et_4N)[Mo_2O_2(SCH_2CH_2O)_3Cl]$, a = 15.387 (1) Å, b = 10.928 (1) Å, c = 14.062 (1) Å, $Pna2_1$, Z = 4; $(Pr_3NH)[Mo_2O_2(SCH_2CH_2O)_3(SCH_2CH_2OH)]$, a = 9.696 (1) Å, b = 10.800 (1) Å, c = 14.401 (1) Å, α = 86.37 (1)°, β = 88.01 (1)°, γ = 65.00 (1)°, $P\bar{1}$, Z = 2.

Introduction

Our interest in thiolate–molybdenum chemistry is related to the possibility of molybdenum–sulfur interactions in various molybdenum-containing enzymes[2] and to the observation that molybdenum and sulfur are still two of the most variable and least predictable elements of the periodic table. Well-characterized oxomolybdenum(V) species contain[2,3] the $[MoO]^{3+}$, $[Mo_2O_2X]^{4+}$, and $[Mo_2O_2X_2]^{2+}$ (X = O, S) structural units (Figure 1a–c; syn isomers only are shown for the binuclear structures). Recently, a new triply bridged structural unit (Figure 1d) has emerged.[4-6] It can be described as two square-pyramidal $[MoO]^{3+}$ units sharing an edge of their basal coordination planes, with another bridging ligand, Z, bound approximately trans to both terminal oxo ligands.

We have recently described[7-9] the syntheses and structures of the first well-characterized mononuclear and binuclear oxomolybdenum(V) species containing monodentate thiolate ligands, $[MoO(SAr)_4]^-$ and $[Mo_2O_4(SR)_4]^{2-}$. Particular points of interest are the following: (i) the observation[7] of an intense electronic absorption at about 600 nm in $[MoO(SAr)_4]^-$; the molybdo enzymes xanthine oxidase and sulfite oxidase feature[10,11] similar absorptions; (ii) the occurrence[8] in the binuclear salt $(Me_4N)_2[Mo_2O_4(SPh)_4]$ of two structural isomers differing in the orientation of S–C vectors; abnormally small S–Mo–S bond angles in one of the isomers appear to indicate attractive interactions between the sulfur atoms of "monodentate" benzenethiolate ligands.

We now report the systematic syntheses of the triply bridged oxomolybdenum(V) species $[Mo_2O_2(SR)_7]^-$ and $[Mo_2O_2(SR)_6Z]^-$ (Z = OR′, NR′$_2$) containing monodentate thiolate ligands and the formation of three homologous complexes involving the 2-oxoethanethiolate ligand, $(Et_4N)[Mo_2O_2(SCH_2CH_2O)_2Cl_3]$, $(Et_4N)[Mo_2O_2(SCH_2CH_2O)_3Cl]$, and $(Pr_3NH)[Mo_2O_2(SCH_2CH_2O)_3(SCH_2CH_2OH)]$, together with the crystal structures of the latter three compounds.

Previous reports on the 2-hydroxyethanethiol–molybdenum(V) system include two compounds formulated[12] as $[Mo_2O_4(SCH_2CH_2OH)_2]$ and $[Mo_2O_3(SCH_2CH_2OH)_4]$, but structural information is not available. Newton[13] has briefly described the conversion of the dioxo bridge in $[Mo_2O_4(S_2CNEt_2)_2]$ to an apparent triple bridge in $[Mo_2O_3(SCH_2CH_2O)(S_2CNEt_2)_2]$ and Enemark, Haight, and coworkers published[4] the crystal structure of the related $[Mo_2O_3(SCH_2CH_2O)(Ox)_2]$ (oxH = 8-hydroxyquinoline), which was the first structural confirmation of the existence of a triple bridge. Another example of the bridge involving 2-oxoethanethiolate, in $[Mo_2O_2S(SCH_2CH_2O)(S_2CNEt_2)_2]$, was recently revealed.[14]

Experimental Section

Synthesis. All solutions used in the syntheses and the physical measurements were flushed with purified dinitrogen. Solvents and reagents were analytical reagent grade and were dried before use; in the syntheses with 2-hydroxyethanethiol the normal concentrations of water in reagent acetonitrile and alcohols do not appear to influence the preparations. Microanalyses were performed by the Australian Microanalytical Service, Alfred Bernhardt Mikroanalytisches Laboratorium, and the Microanalytical Laboratory of the University of N.S.W. Analytical data are listed in Supplementary Table S1.

Yellow $(Et_4N)_2[MoO_2(NCS)_4]$, prepared by the method of Brisdon and Edwards,[15] was observed to undergo during a period of 1 week the known spontaneous solid-state reaction which produces a maroon solid. This maroon compound, which is not well characterized, is presumed to be a binuclear oxo(thiocyanato)molybdate(V) complex. Despite this uncertainty, the mixture of maroon plus yellow solids is a useful chloride-free precursor in reactions with thiols, which complete the reduction of any residual Mo(VI) species.

Tetraethylammonium Aquotetrachlorooxomolybdate(V), $(Et_4N)[MoOCl_4(OH_2)]$. Dry HCl was passed into a suspension of ammonium molybdate in ethanol for about 3 h. The resulting emerald green solution was stirred for 24 h and filtered, and a small molar excess (relative to Mo) of Et_4NCl added. The product which crystallized after volume reduction was filtered off and vacuum dried over KOH.

Tetraethylammonium Trichloro-μ-(2-oxoethanethiolato-*S*,μ-*O*)-μ-(2-oxoethanethiolato-μ-*S*,μ-*O*)bis(oxomolybdate(V)), $(Et_4N)[Mo_2O_2(SCH_2CH_2O)_2Cl_3]$ (I). $(Et_4N)[MoOCl_4(OH_2)]$ (4.0 g, 9.95

0020-1669/79/1318-1875$01.00/0

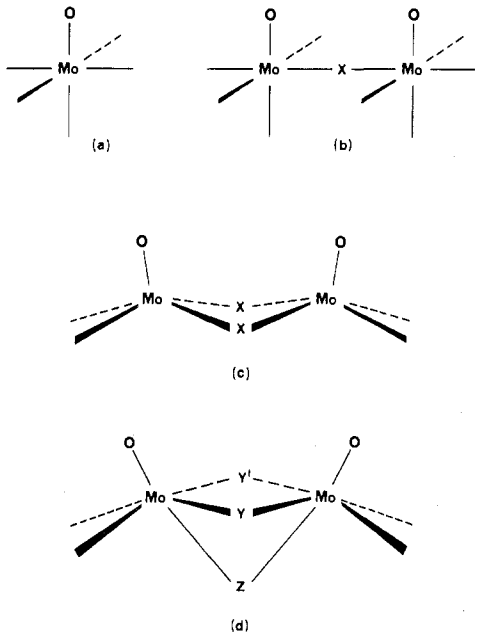

Figure 1.

mmol) was dissolved in 1-butanol (100 cm^3) at 95 °C. A solution of $HOCH_2CH_2SH$ (0.78 g, 9.95 mmol) and Pr_3N (2.85 g, 19.9 mmol) in 1-butanol (30 cm^3) was added slowly with stirring, resulting in the formation of a yellow microcrystalline product. The mixture was cooled to 0 °C for several hours, and then the product was filtered, washed with 1-butanol, and vacuum dried; yield 2.6 g (85%). This compound is soluble in acetone and acetonitrile but sparingly soluble in alcohols; it can be recrystallized from hot acetonitrile or from acetonitrile–alcohol mixtures.

In acetonitrile solution $(Et_4N)[Mo_2O_2(SCH_2CH_2O)_2Cl_3]$ is not very susceptible to oxidation by dioxygen but is decomposed by hydrochloric acid, strong base, or hydrogen sulfide. It undergoes base-catalyzed reactions with thiols.

Tetraethylammonium Chloro-μ-(2-oxoethanethiolato-*S*,μ-*O*)-μ-(2-oxoethanethiolato-μ-*S*,μ-*O*)-(2-oxoethanethiolato-*S*,*O*)bis(oxomolybdate(V)), $(Et_4N)[Mo_2O_2(SCH_2CH_2O)_3Cl]$ (II). A reproducible synthetic procedure for this compound has not yet been developed. The well-formed crystals used for the structure determination were obtained from a reaction of $(Et_4N)[MoOCl_4(OH_2)]$, $HOCH_2CH_2SH$, and Pr_3N, 1:1:2 molar ratio, dissolved in a mixture of methanol, 1-propanol, and a small proportion of acetonitrile. When the normal product of such reactions, $(Et_4N)[Mo_2O_2(SCH_2CH_2O)_2Cl_3]$, did not crystallize as expected, further $HOCH_2CH_2SH$ and Pr_3N were added until the molar ratios were 1:3:3. The orange-yellow crystals that developed overnight were filtered off, washed with a little 1-propanol, and vacuum dried. Subsequent attempts to repeat this preparation have yielded different products, as have reactions with the stoichiometric ratio (2:3:6) of $(Et_4N)[MoOCl_4(OH_2)]$, $HOCH_2CH_2SH$, and Pr_3N.

Tripropylammonium μ-(2-Oxoethanethiolato-*S*,μ-*O*)-μ-(2-oxoethanethiolato-μ-*S*,μ-*O*)-(2-oxoethanethiolato-*S*,*O*)(2-hydroxyethanethiolato)bis(oxomolybdate(V)), $(Pr_3NH)[Mo_2O_2(SCH_2CH_2O)_3(SCH_2CH_2OH)]$ (III). The maroon tetraethylammonium oxo(thiocyanato)molybdate(V) compound (see above) (3.05 g) dissolved in acetonitrile (25 cm^3) plus methanol (25 cm^3) was added to a solution of $HOCH_2CH_2SH$ (2.5 g) and Pr_3N (4.6 g) in ethanol (25 cm^3) at room temperature. The solution changed color slightly from red-brown to orange during 2 weeks, after which the solvents were removed under vacuum. The red oil was dissolved in 1-propanol (10 cm^3) and ethanol (25 cm^3) and stored at 0 °C. Well-developed yellow crystals grew slowly in very small but reproducible yield. The crystals were separated and vacuum dried; they are soluble in common alcohols and aprotic solvents.

Tetraethylammonium Heptakis(benzylthiolato)bis(oxomolybdate(V)), $(Et_4N)[Mo_2O_2(SCH_2Ph)_7]$. $PhCH_2SH$ (1.17 cm^3, 9.93 mmol) and Et_3N (1.38 cm^3, 9.93 mmol) were dissolved in DMF (6 cm^3) and added slowly to solid $[MoOCl_3(THF)_2]$[7] (0.9 g, 2.5 mmol) to give a transient purple coloration which rapidly turned red. The solution was filtered and stirred for 1 h. Et_4NI (0.8 g, 3.1 mmol) in methanol (25 cm^3) was added dropwise and the red crystalline product filtered off, washed with methanol, and vacuum dried. Recrystallization can be effected from DMF/MeOH mixtures. Substitution of Et_4N^+ by Ph_4As^+ or $MePh_3P^+$ leads to the corresponding salts.

Table I. Compounds $B[Mo_2O_2(SR)_6Z]$ Isolated[a]

B	R	Z	yield, %
Et_4N	CH_2Ph	SCH_2Ph	60
Ph_4As	CH_2Ph	SCH_2Ph	60
Et_4N	$^1/_2$ $(-(CH_2)_3-)$	OMe[b]	low
Ph_4As	$^1/_2$ $(-(CH_2)_2-)$	OMe[b]	low
Et_3NH	Ph	OMe[c]	47
Et_4N	Ph	OMe	89
Ph_3PNPPh_3	Ph	OMe	60
Et_4N	Ph	OEt	50
Et_4N	Ph	O-*i*-Pr	55
Et_4N	*p*-MeC_6H_4	OMe	50
Ph_3MeP	*p*-MeC_6H_4	OMe	25
Et_4N	*p*-MeC_6H_4	OEt	51
Et_4N	Ph	NEt_2	60
Et_4N	*p*-MeC_6H_4	NEt_2	45
Et_4N	Ph	N-*n*-Pr_2	40

[a] Analytical data are listed in Supplementary Table S1. [b] These compounds were not obtained analytically pure. [c] Contains one molecule of methanol in the crystal.

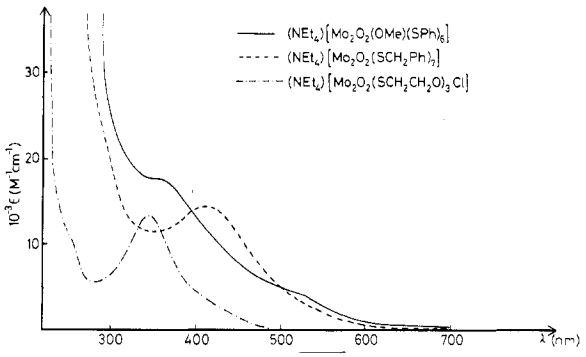

Figure 2. Electronic spectra of $(Et_4N)[Mo_2O_2(SCH_2Ph)_7]$ (DMF solution), $(Et_4N)[Mo_2O_2(SPh)_6(OMe)]$ (MeCN solution), and $(Et_4N)[Mo_2O_2(SCH_2CH_2O)_3Cl]$ (MeCN solution).

Similar procedures with the alkylthiols RSH (R = Et, *n*-Pr, *i*-Pr, *t*-Bu, and C_6H_{11}) and $HS(CH_2)_nSH$ (n = 2, 3) also produce red solutions, but isolation of solid products has not been achieved, except for the dithiols where low yields (25%) of slightly impure $B[Mo_2O_2(S(CH_2)_nS)_3(OMe)]$ (B = Et_4N, Ph_4As) were obtained.

Tetraethylammonium Hexakis(benzenethiolato)methoxybis(oxomolybdate(V)), $(Et_4N)[Mo_2O_2(SPh)_6(OCH_3)]$. Et_3N (5.08 cm^3, 36.4 mmol) and PhSH (3.8 cm^3, 36.4 mmol) were dissolved in acetonitrile (10 cm^3) and the solution was added dropwise to $[MoOCl_3(THF)_2]$ (3.3 g, 9.1 mmol) combined with acetonitrile (25 cm^3). The deep blue solution was filtered and reduced in volume by evaporation to 14 cm^3. Et_4NI (2.93 g, 11.4 mmol) in methanol (50 cm^3) was added dropwise at 50 °C and the mixture was stirred at 50–60 °C for 18 h and cooled slowly to −20 °C. The beautiful red-orange crystals were washed with methanol and dried under vacuum. A similar reaction can be effected at room temperature but the reaction time is greatly increased, and the methanol must be added in stages to prevent precipitation of $(Et_4N)[MoO(SPh)_4]$.

Recrystallization can be effected with acetonitrile–methanol mixtures.

If no cation is added, $(Et_3NH)[Mo_2O_2(SPh)_6(OCH_3)]\cdot CH_3OH$ can be isolated. Similar procedures using different cations, alcohols, and *p*-tolylthiol produced the range of analogous compounds listed in Table I.

A stoichiometric quantity of NaOR (R = Me, Et) in the corresponding alcohol can be used as the source of alkoxy ligand and reacts rapidly with $[MoO(SAr)_4]^-$ at room temperature.

Tetraethylammonium Hexakis(benzenethiolato)chlorobis(oxomolybdate(V)), $(Et_4N)[Mo_2O_2(SPh)_6Cl]$. Acetonitrile (20 cm^3) was added at 0 °C to $(Et_4N)[MoO(SPh)_4]$ (1.7 g, 1.03 mmol) and $FeCl_3$

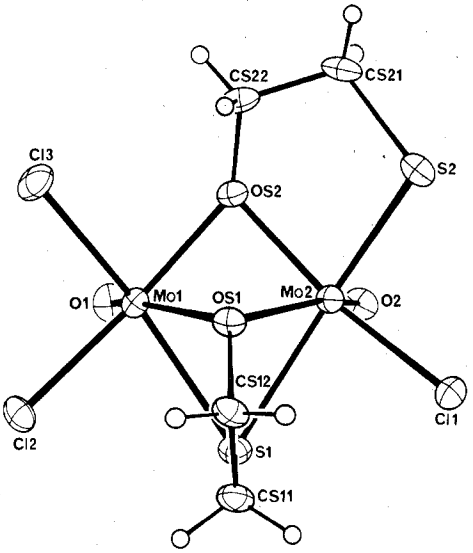

Figure 3. $(Et_4N)[Mo_2O_2(SCH_2CH_2O)_2Cl_3]$, "underside" view of the anion.

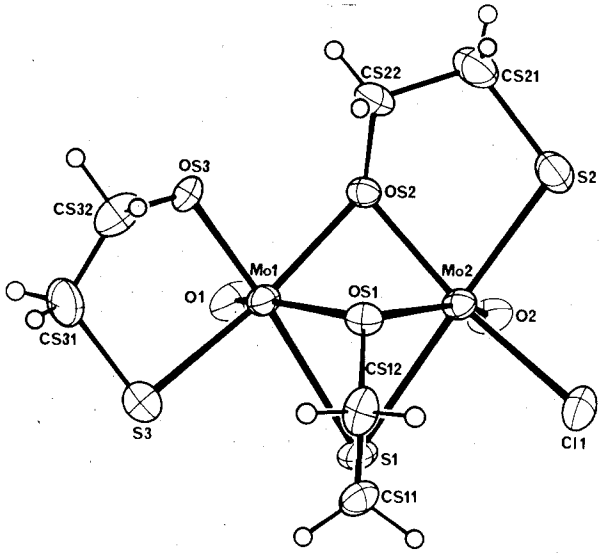

Figure 4. $(Et_4N)[Mo_2O_2(SCH_2CH_2O)_3Cl]$, "underside" view of the anion.

(0.09 g, 0.65 mmol) producing a bright red-orange solution whose electronic spectrum is very similar to that of $[Mo_2O_2(SPh)_6(OCH_3)]^-$ (Figure 2). Immediate and rapid evaporation of the solvent at 0 °C produced a red oil, which was extracted at room temperature with diethyl ether (15 cm^3) producing an orange powder. This was dissolved in acetonitrile (5 cm^3) at 0 °C, and the solution was filtered and treated as just described. The orange powder was washed with diethyl ether and dried under vacuum. Attempted recrystallization led to an insoluble brown solid.

The IR spectrum of the orange solid exhibited bands at 948 and 957 cm^{-1}. Anal. Calcd for $(Et_4N)[Mo_2O_2(SPh)_6Cl](FeCl_2)_{0.1}$: C, 49.98; H, 4.77; Cl, 4.02; Fe, 0.53; N, 1.33; O, 3.06; S, 18.2. Found: C, 49.64; H, 4.64; Cl, 4.6; Fe, 0.5; N, 1.12; O, 3.42; S, 17.2. PhSSPh (identified by melting point and IR and mass spectra) was recovered from the first diethyl ether extract. Extraction of the red oil with alcohols R'OH (R' = Me, Et, *i*-Pr) provides another route to the salts $B[Mo_2O_2(SAr)_6(OR')]$.

Tetraethylammonium Hexakis(benzenethiolato)(diethylamido)-bis(oxomolybdate(V)), $(Et_4N)[Mo_2O_2(SPh)_6(NEt_2)]$. Addition of 1.5 molar equiv of dry, distilled Et_2NH to the red-orange solution described above, before the evaporation and extraction, allows isolation of this compound. Equivalent procedures lead to the other amido salts listed in Table I. All can be recrystallized from acetonitrile–diethyl ether.

X-ray Crystallography. The single crystals of $(Et_4N)[Mo_2O_2(SCH_2CH_2O)_2Cl_3]$, $(Et_4N)[Mo_2O_2(SCH_2CH_2O)_3Cl]$, and $(Pr_3NH)[Mo_2O_2(SCH_2CH_2O)_3(SCH_2CH_2OH)]$ were selected directly from reaction products. All pertinent data and crystallographic results on these crystals are set out in Table II. The following statements outline the general crystallographic procedures adopted and detail anomalies and difficulties that arose. Space groups were determined by Weissenberg photography. Unit-cell dimensions were obtained from reflections (9/crystal) centered on a Siemens diffractometer with the radiation specified in Table II. There were no significant diminutions of intensities of standard reflections (1/crystal) monitored every 22 reflections. The standard deviation of relative intensity (I = Np − Nb) was calculated as $\sigma(I) = [Np + Nb + (0.04Np)^2]^{1/2}$, where Np and Nb are the integrated peak and background counts, respectively. Diffraction data for $(Et_4N)[Mo_2O_2(SCH_2CH_2O)_3Cl]$ were not observable beyond $(\sin\theta)/\lambda = 0.6$.

All data were corrected for absorption, calculated by numerical integration over a 5 × 5 × 5 grid. In the case of $(Pr_3NH)[Mo_2O_2(SCH_2CH_2O)_3(SCH_2CH_2OH)]$ three of the six crystal surfaces were not lattice planes but fracture surfaces, which for the purposes of absorption calculation were approximated by lattice planes. The resulting reduced precision in the absorption corrections is apparent in small but systematic discrepancies in the final structure factors.

The structures were solved with standard heavy atom and direct methods procedures. At appropriate stages in the least-squares refinement (minimizing $\sum w(|F_o| - |F_c|)^2$, with $w = (\sigma(F))^{-2}$) all methylene hydrogen atoms were included and maintained at idealized positions (d_{C-H} = 0.95 Å). The temperature factors of all hydrogen atoms were maintained throughout the refinements as the isotropic equivalents of the temperature factors of the atoms to which they were bonded. In $(Et_4N)[Mo_2O_2(SCH_2CH_2O)_2Cl_3]$ all 12 methyl hydrogen atoms were located in difference syntheses, and their positions allowed unconstrained variation in the least-squares refinement. In $(Pr_3NH)[Mo_2O_2(SCH_2CH_2O)_3(SCH_2CH_2OH)]$ the hydrogen atoms bonded to N and OS4 as well as six of the nine methyl hydrogen atoms were located in difference syntheses, and the remaining three hydrogen atoms were then included at idealized positions; the positions of these 11 hydrogen atoms were varied in the least-squares refinement.

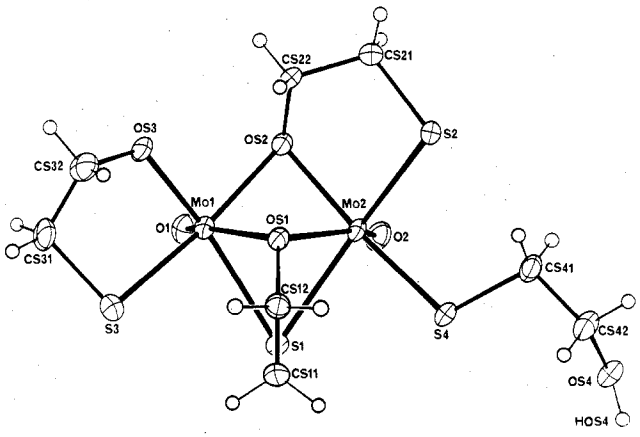

Figure 5. $(Pr_3NH)[Mo_2O_2(SCH_2CH_2O)_3(SCH_2CH_2OH)]$, "underside" view of the anion.

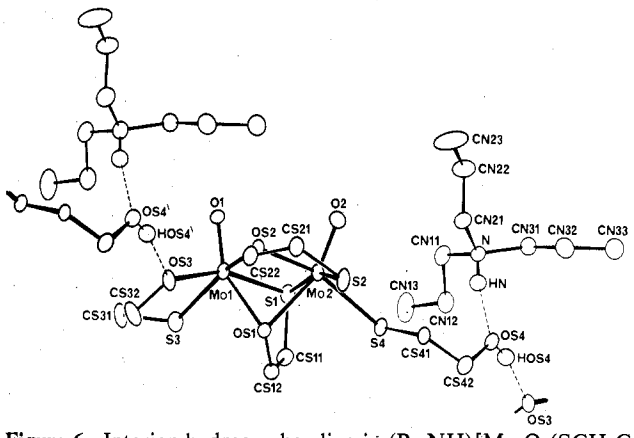

Figure 6. Interion hydrogen bonding in $(Pr_3NH)[Mo_2O_2(SCH_2CH_2O)_3(SCH_2CH_2OH)]$.

Table II. Crystallographic Details[a]

	I $Mo_2O_4Cl_3S_2NC_{12}H_{26}$	II $Mo_2O_5ClS_3NC_{14}H_{32}$	III $Mo_2O_6S_4NC_{17}H_{39}$
a, Å	12.877 (1)	15.387 (1)	9.696 (1)
b, Å	15.351 (1)	10.928 (1)	10.800 (1)
c, Å	13.147 (1)	14.062 (1)	14.401 (1)
α, deg	90	90	86.37 (1)
β, deg	122.76 (1)	90	88.01 (1)
γ, deg	90	90	65.00 (1)
V, Å^3	2185.5	2364.6	1363.97
space group	$P2_1/c$	$Pna2_1$	$P\bar{1}$
Z	4	4	2
d_{obsd}, g cm^{-3}	1.84 (3)	1.74 (2)	1.65 (2)
d_{calcd}, g cm^{-3}	1.86	1.74	1.64
$F(000)$	1224	1248	688
radiation used	Cu Kα, 1.5418 Å	Mo Kα, 0.710 69 Å	Cu Kα, 1.5418 Å
μ, cm^{-1}	150.1	14.29	107.8
θ_{max}, deg	70	25	70
no. of intens measurements	4350	2174	5207
no. of independent data	4162	2173	5192
$I/\sigma(I)$[b]	>2.58	>1	>2.58
no. of data in refinement, n	3655	1580	4734
no. of variable parameters, m	255	234	305
$R_1 = \Sigma^n\|\|F_o\| - \|F_c\|\|/\Sigma^n\|F_o\|$	0.043	0.062	0.054
$R_2 = [\Sigma^n w(\|F_o\| - \|F_c\|)^2/\Sigma^n w\|F_o\|^2]^{1/2}$	0.054	0.051	0.070
$[\Sigma^n w(\|F_o\| - \|F_c\|)^2/(n-m)]^{1/2}$	2.05	1.07	2.89
cryst dimensions (max/min), cm	0.022/0.015	0.025/0.016	0.030/0.019
Larson extinction parameter, 10^6 g	43 (9)	0	173 (24)
transmission factor (min/max)	0.040/0.262	0.723/0.866	0.058/0.300

[a] In this table and following tables I = $(Et_4N)[Mo_2O_2(SCH_2CH_2O)_2Cl_3]$, II = $(Et_4N)[Mo_2O_2(SCH_2CH_2O)_3Cl]$, and III = $(Pr_3NH)[Mo_2O_2(SCH_2CH_2O)_3(SCH_2CH_2OH)]$. [b] Criterion for inclusion of data in refinement.

The three structures comprise a homologous series, and a consistent atom labeling scheme is used (see Figures 3–6). Within each ligand the atoms are labeled Sn–CSn1–CSn2–OSn. Ligand 1 (n = 1) doubly bridges the two molybdenum atoms, ligand 2 chelates Mo2, with OS2 bridging Mo2 and Mo1, ligand 3 in two structures chelates Mo1 and in the other is replaced by Cl2 and Cl3, and Cl1 or ligand 4 (at S4) is coordinated to Mo2. Carbon atoms in the alkyl chains (p) of the quaternary ammonium cations are labeled CNpq, with q increasing away from N. All hydrogen atoms are labeled H$hxxxx$, where h = 1, 2, or 3 and $xxxx$ is the label of the atom to which hydrogen is bonded.

In both structures containing chelate ring 3 the vibrations of the methylene carbon atoms indicated the possibility of disorder between locations approximately perpendicular to the Mo1, S3, OS3 plane. The separation of alternative locations for these atoms was more pronounced in $(Et_4N)[Mo_2O_2(SCH_2CH_2O)_3Cl]$, and a model involving equal occurrence of approximately enantiomorphic skew conformations of the dimethylene chain was refinable. However, in view of the separations (~0.6–0.8 Å) of the disordered locations, the limited sphere of diffraction data available, and the fact that the purpose of the analysis was to determine the primary features of the coordination geometry, further modeling of the disorder was not undertaken.

The scattering factors were those of uncharged atoms, taken from standard compilations.[16] Real and imaginary components of anomalous scattering were incorporated for Mo, S, and Cl atoms, except that the real components only for S and Cl were included in the less precise structure, $(Et_4N)[Mo_2O_2(SCH_2CH_2O)_3Cl]$. No attempt was made to determine the absolute configuration of $(Et_4N)[Mo_2O_2(SCH_2CH_2O)_3Cl]$; Friedel pairs were not measured.

Larson's[17] isotropic correction for secondary extinction was included and refined for $(Et_4N)[Mo_2O_2(SCH_2CH_2O)_2Cl_3]$ and $(Pr_3NH)[Mo_2O_2(SCH_2CH_2O)_3(SCH_2CH_2OH)]$; in $(Et_4N)[Mo_2O_2(SCH_2CH_2O)_3Cl]$ the parameter g refined to an insignificant negative value, and therefore was set to zero.

In difference maps calculated after least-squares refinement there were no peaks of chemical significance, the largest features (all less than 1.2 e Å^{-3}) occurring close to the molybdenum atoms. The structure factor discrepancies for $(Pr_3NH)[Mo_2O_2(SCH_2CH_2O)_3(SCH_2CH_2OH)]$ are not randomly distributed, which is regarded as a consequence of insufficient precision in the absorption corrections.

Listings of F_o and F_c for the three crystals are included with the supplementary material, as Tables S2, S3, and S4.

In the final least-squares cycle for each structure all positional parameters were blocked together, and consequently all positional parameter covariance is included in the estimates of errors in interatomic distances and angles.

Positional parameters and their estimated standard deviations are listed in Tables III, IV, and V. Complete listings of final thermal parameters are available with the supplementary material in Tables S5, S6, and S7.

Table VI contains the bond distances and Table VII the bond angles of the three anionic complexes; structurally equivalent values resulting from the $Cl^-/^-OCH_2CH_2S^-$ substitution are grouped together. Dimensions of the cations in the three structures are unexceptional and are listed with the supplementary material. Other than the interion hydrogen bonding in $(Pr_3NH)[Mo_2O_2(SCH_2CH_2O)_3(SCH_2CH_2OH)]$ described below, there are no significant intermolecular contacts in the three crystals.

Physical Measurements. Powder diffraction data were obtained with a Philips diffractometer, using Co Kα radiation. Other techniques have been described previously.[7] Normal diamagnetic corrections for ligands, cations, and Mo were applied to measured magnetic susceptibilities.

Results

Syntheses Involving 2-Hydroxyethanethiol. Reactions of 2-hydroxyethanethiol and various Brønsted bases with molybdenum precursors, particularly oxomolybdenum(V) complexes, have yielded many products. Most of these new complexes are yellow, orange, or red, but other strongly colored compounds with lower energy charge-transfer absorption have been observed. Details of all factors influential in the formation and crystallization of particular products are not yet fully understood. While intensive investigations of this system are continuing, we report here only on the title compounds. Powder diffraction data which are most valuable for identification of these compounds are included in Supplementary Table S8.

The complex $(Et_4N)[Mo_2O_2(SCH_2CH_2O)_2Cl_3]$ with three terminal chloride ligands is only sparingly soluble in alcohols, whereas the other complexes are much more soluble. Crystallization of the trichloro complex can therefore be used to monitor its occurrence in reaction mixtures. $(Et_4N)[Mo_2O_2(SCH_2CH_2O)_2Cl_3]$ crystallizes in 80% yield from a 1:5 $MoOCl_4$–$HOCH_2CH_2SH$ mixture in 1-butanol without

Table III. Fractional Atomic Coordinates and Estimated Standard Deviations for $(Et_4N)[Mo_2O_2(SCH_2CH_2O)_2Cl_3]$

atom	*x*	*y*	*z*	atom	*x*	*y*	*z*
Mo1	0.97738 (3)	0.83915 (3)	0.15125 (3)	H1CS11	1.1962 (0)	0.6896 (0)	0.4575 (0)
Mo2	1.22851 (3)	0.85185 (2)	0.27808 (3)	H2CS11	1.0527 (0)	0.6803 (0)	0.3845 (0)
Cl1	1.3912 (1)	0.8043 (1)	0.4722 (1)	H1CS12	1.0379 (0)	0.8137 (0)	0.4307 (0)
Cl2	0.8355 (1)	0.7602 (1)	0.1801 (1)	H2CS12	1.1786 (0)	0.8225 (0)	0.5037 (0)
Cl3	0.8389 (1)	0.9581 (1)	0.1048 (2)	H1CS21	1.2443 (0)	1.0451 (0)	0.1559 (0)
S1	1.1158 (1)	0.7139 (1)	0.2548 (1)	H2CS21	1.2388 (0)	1.1143 (0)	0.2409 (0)
S2	1.3338 (1)	0.9872 (1)	0.3509 (1)	H1CS22	1.0790 (0)	1.0425 (0)	0.2313 (0)
O1	0.9433 (3)	0.7987 (3)	0.0184 (3)	H2CS22	1.0425 (0)	1.0521 (0)	0.0969 (0)
O2	1.2691 (3)	0.8107 (3)	0.1862 (4)	H1CN11	0.4653 (0)	0.9803 (0)	0.6956 (0)
OS1	1.1000 (3)	0.8677 (2)	0.3395 (3)	H2CN11	0.3370 (0)	0.9728 (0)	0.5843 (0)
OS2	1.0942 (3)	0.9325 (2)	0.1615 (3)	H1CN21	0.3571 (0)	1.1251 (0)	0.5504 (0)
CS11	1.1199 (5)	0.7137 (4)	0.3940 (5)	H2CN21	0.4821 (0)	1.1242 (0)	0.6646 (0)
CS12	1.1085 (5)	0.8080 (4)	0.4263 (5)	H1CN31	0.1962 (0)	1.1434 (0)	0.6504 (0)
CS21	1.2287 (6)	1.0540 (4)	0.2183 (6)	H2CN31	0.1859 (0)	1.0502 (0)	0.6751 (0)
CS22	1.0989 (5)	1.0265 (3)	0.1736 (5)	H1CN41	0.3729 (0)	1.0584 (0)	0.8568 (0)
N	0.3507 (4)	1.0749 (3)	0.6926 (4)	H2CN41	0.3913 (0)	1.1518 (0)	0.8357 (0)
CN11	0.3803 (5)	0.9834 (4)	0.6705 (5)	H1CN12	0.2656 (68)	0.9097 (55)	0.6988 (65)
CN12	0.3513 (9)	0.9123 (5)	0.7288 (8)	H2CN12	0.4017 (64)	0.9067 (57)	0.8076 (70)
CN21	0.3978 (5)	1.1370 (4)	0.6361 (6)	H3CN12	0.3755 (67)	0.8519 (55)	0.7037 (71)
CN22	0.3836 (8)	1.2328 (5)	0.6525 (9)	H1CN22	0.4454 (65)	1.2464 (55)	0.7333 (74)
CN31	0.2130 (5)	1.0860 (5)	0.6344 (6)	H2CN22	0.3051 (69)	1.2499 (56)	0.6338 (69)
CN32	0.1330 (6)	1.0688 (5)	0.5006 (6)	H3CN22	0.4224 (66)	1.2690 (57)	0.6215 (71)
CN41	0.4107 (5)	1.0934 (4)	0.8250 (5)	H1CN32	0.0474 (57)	1.0774 (46)	0.4571 (57)
CN42	0.5487 (6)	1.0810 (6)	0.9006 (7)	H2CN32	0.1566 (56)	1.1012 (48)	0.4625 (59)
				H3CN32	0.1396 (56)	1.0164 (48)	0.4770 (58)
				H1CN42	0.5774 (60)	1.0937 (51)	0.9769 (67)
				H2CN42	0.5938 (60)	1.0295 (52)	0.9013 (61)
				H3CN42	0.5897 (63)	1.1186 (53)	0.8775 (64)

Table IV. Fractional Atomic Coordinates and Estimated Standard Deviations for $(Et_4N)[Mo_2O_2(SCH_2CH_2O)_3Cl]$

atom	*x*	*y*	*z*	atom	*x*	*y*	*z*
Mo1	0.4464 (1)	0.1082 (1)	0.6416 (1)	H1CS11	0.2903 (0)	0.3044 (0)	0.5268 (0)
Mo2	0.4181 (1)	0.2713 (1)	0.7854 (0)	H2CS11	0.2738 (0)	0.3954 (0)	0.6095 (0)
Cl1	0.3439 (3)	0.4632 (4)	0.7964 (3)	H1CS12	0.4211 (0)	0.3675 (0)	0.5166 (0)
S1	0.3042 (2)	0.2048 (3)	0.6698 (3)	H2CS12	0.4044 (0)	0.4589 (0)	0.5957 (0)
S2	0.5336 (3)	0.3765 (4)	0.8642 (3)	H1CS21	0.6738 (0)	0.2944 (0)	0.8623 (0)
S3	0.4028 (3)	0.0967 (5)	0.4809 (4)	H2CS21	0.6105 (0)	0.2023 (0)	0.9110 (0)
O1	0.4095 (6)	−0.0260 (8)	0.6849 (8)	H1CS22	0.6252 (0)	0.2415 (0)	0.7166 (0)
O2	0.3646 (6)	0.1902 (9)	0.8692 (7)	H2CS22	0.6439 (0)	0.1179 (0)	0.7696 (0)
OS1	0.4592 (4)	0.3084 (7)	0.6417 (7)	H1CS31	0.5063 (0)	−0.0418 (0)	0.4273 (0)
OS2	0.5170 (5)	0.1550 (8)	0.7578 (5)	H2CS31	0.5166 (0)	0.0797 (0)	0.3731 (0)
OS3	0.5644 (5)	0.0813 (8)	0.5841 (6)	H1CS32	0.6264 (0)	0.0319 (0)	0.4823 (0)
CS11	0.3098 (9)	0.3299 (14)	0.5882 (11)	H2CS32	0.6000 (0)	0.1551 (0)	0.4762 (0)
CS12	0.4022 (10)	0.3737 (13)	0.5810 (11)	H1CN11	0.3020 (0)	0.4942 (0)	0.1814 (0)
CS21	0.6174 (10)	0.2576 (18)	0.8591 (10)	H2CN11	0.3962 (0)	0.4869 (0)	0.1926 (0)
CS22	0.6086 (8)	0.1898 (14)	0.7678 (10)	H1CN21	0.2120 (0)	0.3249 (0)	0.1067 (0)
CS31	0.5067 (13)	0.0457 (27)	0.4342 (14)	H2CN21	0.2704 (0)	0.3126 (0)	0.0236 (0)
CS32	0.5750 (11)	0.0792 (21)	0.4957 (16)	H1CN31	0.4198 (0)	0.1813 (0)	0.1091 (0)
N	0.3460 (7)	0.3250 (10)	0.1526 (9)	H2CN31	0.4344 (0)	0.2935 (0)	0.0481 (0)
CN11	0.3523 (15)	0.4595 (18)	0.1502 (25)	H1CN41	0.3304 (0)	0.1961 (0)	0.2503 (0)
CN12	0.3631 (14)	0.5228 (17)	0.0498 (13)	H2CN41	0.3784 (0)	0.2920 (0)	0.2867 (0)
CN21	0.2628 (13)	0.2824 (22)	0.0868 (13)				
CN22	0.2453 (13)	0.1525 (19)	0.0841 (15)				
CN31	0.4272 (14)	0.2677 (19)	0.1117 (15)				
CN32	0.5080 (10)	0.2960 (19)	0.1701 (23)				
CN41	0.3261 (17)	0.2840 (23)	0.2489 (14)				
CN42	0.2460 (15)	0.3287 (28)	0.3063 (19)				

added base, indicating the strong acidity of both the alcohol and thiol protons of coordinated 2-hydroxyethanethiol. The complex also crystallizes in high yield (86%) from the stoichiometric reaction 2:2:4 $MoOCl_4^-$–$HOCH_2CH_2SH$–Pr_3N. However, solutions containing small excesses of deprotonated ligand, such as the mixture 2:3:6 $MoOCl_4^-$–$HOCH_2CH_2SH$–Pr_3N in 1-propanol yield no $(Et_4N)[Mo_2O_2(SCH_2CH_2O)_2Cl_3]$, indicating that the terminal chloride ligands are quite unstable, thermodynamically, to substitution by deprotonated 2-hydroxyethanethiol. $(Et_4N)[Mo_2O_2(SCH_2CH_2O)_2Cl_3]$ is formed in high yield when $HOCH_2CH_2SH$ is added to the red-brown basic compounds formed when Pr_3N is added to $(Et_4N)[MoOCl_4(OH_2)]$ in undried solvents.

The compound $(Et_4N)[Mo_2O_2(SCH_2CH_2O)_3Cl]$ was obtained in good yield as well-formed crystals in only one reaction. Solutions containing the stoichiometrically appropriate combination of $(Et_4N)[MoOCl_4(OH_2)]$, $HOCH_2CH_2SH$, and Pr_3N in fact yield other compounds, which will be described in subsequent publications. The complex anion $[Mo_2O_2(SCH_2CH_2O)_3(SCH_2CH_2OH)]^-$ forms salts very soluble in alcohols and polar aprotic solvents commonly used, and it has not yet been crystallized from stoichiometric reaction mixtures using $(Et_4N)[MoOCl_4(OH_2)]$. The hydrogen-bonded salt

Table V. Fractional Atomic Coordinates and Estimated Standard Deviations for $(Pr_3NH)[Mo_2O_2(SCH_2CH_2O)_3(SCH_2CH_2OH)]$

atom	x	y	z	atom	x	y	z
Mo1	0.78314 (4)	0.44227 (3)	0.23443 (3)	H1CS11	1.2254 (0)	0.1921 (0)	0.1608 (0)
Mo2	0.87340 (4)	0.16624 (3)	0.22603 (3)	HC2S11	1.1720 (0)	0.3482 (0)	0.1658 (0)
S1	1.0421 (2)	0.2729 (1)	0.2739 (1)	H1CS12	1.0213 (0)	0.3825 (0)	0.0489 (0)
S2	0.7493 (1)	0.0712 (1)	0.1318 (1)	H2CS12	1.0724 (0)	0.2268 (0)	0.0450 (0)
S3	0.9057 (2)	0.5891 (2)	0.1961 (1)	H1CS21	0.5112 (0)	0.1818 (0)	0.1992 (0)
S4	1.1073 (1)	−0.0111 (1)	0.1731 (1)	H2CS21	0.4976 (0)	0.1998 (0)	0.0911 (0)
O1	0.7355 (5)	0.4674 (4)	0.3482 (3)	H1CS22	0.5919 (0)	0.3613 (0)	0.0868 (0)
O2	0.8581 (5)	0.1160 (4)	0.3381 (3)	H2CS22	0.4608 (0)	0.4048 (0)	0.1614 (0)
OS1	0.8858 (4)	0.3167 (3)	0.1174 (3)	H1CS31	0.7665 (0)	0.7945 (0)	0.1162 (0)
OS2	0.6633 (4)	0.3283 (3)	0.2142 (3)	H2CS31	0.6837 (0)	0.7852 (0)	0.2092 (0)
OS3	0.6168 (4)	0.5850 (4)	0.1594 (3)	H1CS32	0.5446 (0)	0.7649 (0)	0.0951 (0)
OS4	1.3124 (4)	−0.3257 (4)	0.1799 (3)	H2CS32	0.6856 (0)	0.6577 (0)	0.0490 (0)
CS11	1.1391 (7)	0.2767 (6)	0.1664 (5)	H1CS41	1.0284 (0)	−0.1103 (0)	0.0590 (0)
CS12	1.0315 (6)	0.3016 (6)	0.0843 (4)	H2CS41	1.0231 (0)	−0.1809 (0)	0.1549 (0)
CS21	0.5551 (7)	0.2003 (6)	0.1431 (5)	H1CS42	1.2191 (0)	−0.3267 (0)	0.0613 (0)
CS22	0.5586 (6)	0.3381 (5)	0.1456 (4)	H2CS42	1.2926 (0)	−0.2262 (0)	0.0582 (0)
CS31	0.7365 (9)	0.7373 (6)	0.1570 (7)	H1CN11	1.2804 (0)	−0.1772 (0)	0.4627 (0)
CS32	0.6396 (9)	0.6899 (8)	0.1070 (7)	H2CN11	1.1860 (0)	−0.0780 (0)	0.3848 (0)
CS41	1.0814 (7)	−0.1469 (5)	0.1157 (4)	H1CN12	1.4962 (0)	−0.2467 (0)	0.3727 (0)
CS42	1.2331 (7)	−0.2611 (6)	0.0959 (4)	H2CN12	1.4074 (0)	−0.1725 (0)	0.2869 (0)
N	1.2296 (6)	−0.2754 (5)	0.3629 (3)	H1CN13	1.481 (12)	−0.0599 (98)	0.4458 (68)
CN11	1.2682 (8)	−0.1649 (6)	0.3971 (5)	H2CN13	1.335 (11)	0.038 (10)	0.3587 (65)
CN12	1.4116 (8)	−0.1667 (7)	0.3518 (5)	H3CN13	1.516 (12)	−0.042 (10)	0.3222 (69)
CN13	1.4371 (13)	−0.0439 (9)	0.3724 (11)	H1CN21	1.0408 (0)	−0.3018 (0)	0.3350 (0)
CN21	1.0631 (7)	−0.2415 (6)	0.3703 (4)	H2CN21	1.0068 (0)	−0.1554 (0)	0.3386 (0)
CN22	1.0025 (9)	−0.2412 (9)	0.4674 (5)	H1CN22	1.0588 (0)	−0.3263 (0)	0.4988 (0)
CN23	0.8389 (12)	−0.2137 (21)	0.4629 (9)	H2CN22	1.0100 (0)	−0.1702 (0)	0.4992 (0)
CN31	1.3300 (7)	−0.4139 (6)	0.4048 (4)	H1CN23	0.792 (14)	−0.236 (12)	0.4268 (81)
CN32	1.3023 (9)	−0.5291 (7)	0.3680 (5)	H2CN23	0.827 (14)	−0.253 (12)	0.5145 (88)
CN33	1.4255 (11)	−0.6661 (8)	0.4000 (7)	H3CN23	0.760 (14)	−0.130 (12)	0.4815 (83)
HN	1.2556 (73)	−0.2764 (63)	0.3051 (44)	H1CN31	1.3172 (0)	−0.4142 (0)	0.4703 (0)
HOS4	1.4044 (74)	−0.3598 (65)	0.1814 (43)	H2CN31	1.4337 (0)	−0.4309 (0)	0.3950 (0)
				H1CN32	1.2066 (0)	−0.5239 (0)	0.3901 (0)
				H2CN32	1.3006 (0)	−0.5214 (0)	0.3021 (0)
				H1CN33	1.5237 (99)	−0.6884 (82)	0.3863 (56)
				H2CN33	1.4092 (95)	−0.7546 (85)	0.3485 (56)
				H3CN33	1.4330 (93)	−0.6940 (82)	0.4813 (57)

Table VI. Bond Lengths (Å)

bond	I	II	III
Mo1-Mo2	2.728 (1)	2.731 (2)	2.739 (1)
Mo1-O1	1.673 (4)	1.686 (9)	1.693 (4)
Mo2-O2	1.678 (4)	1.688 (9)	1.691 (4)
Mo1-S1	2.470 (1)	2.463 (3)	2.462 (1)
Mo2-S1	2.491 (1)	2.498 (4)	2.500 (1)
Mo2-S2	2.381 (1)	2.390 (4)	2.383 (1)
Mo1-OS1	2.140 (3)	2.197 (7)	2.168 (3)
Mo2-OS1	2.212 (3)	2.156 (9)	2.221 (4)
Mo1-OS2	2.028 (3)	2.028 (8)	2.056 (4)
Mo2-OS2	2.001 (3)	2.021 (8)	2.053 (3)
Mo1-S3	-	2.361 (5)	2.381 (2)
Mo1-Cl2	2.387 (1)	-	-
Mo1-OS3	-	2.008 (8)	1.988 (4)
Mo1-Cl3	2.388 (1)	-	-
Mo2-S4	-	-	2.405 (1)
Mo2-Cl1	2.377 (1)	2.392 (4)	-
S1-CS11	1.802 (6)	1.79 (2)	1.791 (7)
S2-CS21	1.835 (7)	1.83 (2)	1.817 (6)
OS1-CS12	1.421 (6)	1.42 (2)	1.421 (6)
OS2-CS22	1.449 (6)	1.47 (1)	1.408 (6)
CS11-CS12	1.538 (8)	1.50 (2)	1.538 (9)
CS21-CS22	1.502 (8)	1.49 (2)	1.507 (8)
S3-CS31		1.82 (2)	1.817 (8)
OS3-CS32		1.26 (2)	1.412 (8)
CS31-CS32		1.41 (2)	1.47 (1)
S4-CS41			1.837 (6)
OS4-CS42			1.430 (7)
CS41-CS42			1.500 (7)
OS4-HOS4			0.81 (7)
N-HN			0.86 (6)
OS4-HN			1.91 (6)
HOS4-OS3			1.91 (7)

$(Pr_3NH)[Mo_2O_2(SCH_2CH_2O)_3(SCH_2CH_2OH)]$ has been crystallized in very small but reproducible yields from the reaction described in the Experimental Section.

Reactions with Alkylthiols. As reported previously,[7,9] the deep blue, mononuclear, square-pyramidal anions $[MoO(SAr)_4]^-$ can be synthesized by the addition of 4 equiv of an equimolar mixture of ArSH (Ar = Ph, *p*-tolyl, C_6Cl_5) and Et_3N in acetonitrile or DMF to a solution of $[MoOCl_3(THF)_2]$.

$$[MoOCl_3(THF)_2] + 4ArSH + 4Et_3N \rightarrow [MoO(SAr)_4]^- + 3Cl^- + 4Et_3NH^+ + 2THF \quad (1)$$

Addition of quaternary cations B^+ in methanol allows isolation of crystalline salts $B[MoO(SAr)_4]$. The use of benzylthiol $PhCH_2SH$ produces a solution (DMF) whose transient blue-purple coloration rapidly changes to red-orange from which the crystalline salts $B[Mo_2O_2(SCH_2Ph)_7]$ (Table I) can be isolated. Other alkylthiols lead to red-orange solutions (DMF) but isolation of solid products has not been successful so far. The electronic spectra of such solutions exhibit an absorption maximum at 400 nm ($\epsilon \sim 20\,000$ cm^{-1} M^{-1}) and are very similar to the solution spectrum of $[Mo_2O_2(SCH_2Ph)_7]^-$ (Table VIII and Figure 2). Therefore it is presumed that $[Mo_2O_2(SR)_7]^-$ anions with other alkylthiols exist in solution. The dithiols $HS(CH_2)_nSH$ (n = 2, 3) produce similar solutions from which low yields of orange crystals were obtained. Their analytical data (Table S1) and physical properties indicated that they were slightly impure samples of $B[Mo_2O_2(S(CH_2)_nS)_3(OCH_3)]$.

Reactions of $[MoO(SAr)_4]^-$ with Sources of Alkoxy Ligands. The mononuclear anions $[MoO(SAr)_4]^-$ can be converted to binuclear species $[Mo_2O_2(SAr)_6Z]^-$ (Z = OR′; R′ = Me, Et, *i*-Pr; see Table I) by the following reactions. (a) Bright red-orange solutions result if solutions of $[MoO(SAr)_4]^-$ in acetonitrile/R′OH (generated from the isolated salt or by

Table VII. Bond Angles (deg)

angle	I	II	III
S1-Mo1-OS2	103.0 (1)	103.7 (2)	104.9 (1)
S1-Mo2-OS2	103.1 (1)	102.7 (2)	103.6 (1)
S1-Mo1-OS1	70.2 (1)	69.7 (2)	69.9 (1)
S1-Mo2-OS1	68.7 (1)	69.6 (2)	68.4 (1)
OS2-Mo1-OS1	73.8 (1)	72.5 (3)	72.2 (1)
OS2-Mo2-OS1	72.8 (1)	73.5 (3)	71.1 (1)
S2-Mo2-OS2	80.6 (1)	80.3 (3)	80.1 (1)
O1-Mo1-OS1	153.6 (2)	153.6 (4)	153.8 (2)
O2-Mo2-OS1	152.9 (2)	153.6 (4)	152.1 (2)
O1-Mo1-S1	89.4 (1)	90.7 (3)	91.7 (2)
O1-Mo1-OS2	95.6 (2)	96.2 (5)	95.9 (2)
O2-Mo2-S1	88.8 (1)	87.7 (3)	90.3 (2)
O2-Mo2-OS2	99.1 (2)	99.8 (4)	98.2 (2)
S1-Mo1-S3 }	-	85.7 (1)	83.8 (1)
S1-Mo1-Cl2 }	84.5 (1)	-	-
S3-Mo1-OS3 }	-	82.2 (3)	82.2 (1)
Cl2-Mo1-Cl3 }	84.2 (1)	-	-
OS3-Mo1-OS2 }	-	83.0 (3)	83.1 (1)
Cl3-Mo1-OS2 }	84.3 (1)	-	-
S1-Mo2-Cl1 }	89.3 (1)	87.8 (1)	-
S1-Mo2-S4 }	-	-	84.0 (1)
S2-Mo2-Cl1 }	81.8 (1)	84.4 (2)	-
S2-Mo2-S4 }	-	-	86.0 (1)
O1-Mo1-S3 }	-	101.8 (4)	103.8 (2)
O1-Mo1-Cl2 }	100.7 (1)	-	-
O1-Mo1-OS3 }	-	108.8 (4)	107.8 (2)
O1-Mo1-Cl3 }	106.2 (1)	-	-
O2-Mo2-S2	106.6 (1)	107.0 (4)	107.8 (2)
O2-Mo2-Cl1 }	102.7 (1)	100.5 (3)	-
O2-Mo2-S4 }	-	-	103.7 (2)
Mo1-S1-Mo2	66.7 (1)	66.8 (1)	67.0 (1)
Mo1-OS2-Mo2	85.2 (1)	84.9 (3)	83.6 (1)
Mo1-OS1-Mo2	77.6 (1)	77.7 (3)	77.2 (1)
Mo1-S1-CS11	100.2 (2)	100.5 (5)	100.3 (2)
Mo2-S1-CS11	100.5 (2)	99.3 (5)	100.7 (2)
Mo1-OS1-CS12	119.0 (3)	116.4 (7)	119.4 (3)
Mo2-OS1-CS12	118.3 (3)	118.5 (7)	118.4 (3)
Mo2-S2-CS21	98.0 (2)	99.4 (5)	99.0 (2)
Mo1-OS2-CS22	134.1 (3)	131.1 (7)	132.0 (3)
Mo2-OS2-CS22	124.4 (3)	122.8 (8)	122.3 (3)
Mo1-S3-CS31		96.4 (6)	96.6 (2)
Mo1-OS3-CS32		121.3 (9)	121.3 (4)
Mo2-S4-CS41			113.7 (2)
CS42-OS4-HOS4			121 (4)
OS4-HOS4-OS3			167 (6)
N-HN-OS4			165 (6)

Table VIII. Electronic Spectra

compound	solvent	abs max, nm	extinction coeff, M^{-1} cm^{-1}
$(Et_4N)[Mo_2O_2(SCH_2Ph)_7]$	DMF	408	14 500
$(Et_4N)[Mo_2O_2(SPh)_6(OMe)]$	CH_3CN	505 sh	
		360 sh	17 400
		318 sh	
		258 sh	61 500
$(Et_4N)[Mo_2O_2(S\text{-}p\text{-}tolyl)_6(OMe)]$	CH_3CN	515 sh	
		360	20 100
		312 sh	
		260	64 800
$(Et_4N)[Mo_2O_2(SCH_2CH_2O)_2Cl_3]$	CH_3CN	342	10 950
		232 sh	
$(Et_4N)[Mo_2O_2(SCH_2CH_2O)_3Cl]$	CH_3CN	410 sh	
		344	13 300
		249 sh	

reaction 1) are stirred at 50–60 °C for at least 18 h (eq 2). The crystalline salts $B[Mo_2O_2(SAr)_6(OR')]$ can be isolated in high yield. Reactions at room temperature are much slower.

$$2[MoO(SAr)_4]^- + R'OH \rightarrow [Mo_2O_2(SAr)_6(OR')]^- + ArS^- + ArSH \quad (2)$$

(b) Alkoxide ions react directly with $[MoO(SAr)_4]^-$ solutions, although excess reagent destroys the product.

$$2[MoO(SAr)_4]^- + R'O^- \rightarrow [Mo_2O_2(SAr)_6(OR')]^- + 2ArS^- \quad (3)$$

Reactions of $[MoO(SAr)_4]^-$ with $FeCl_3$. $[MoO(SAr)_4]^-$ does not react with $[FeCl_4]^{2-}$ but does with $FeCl_3$ in acetonitrile. A bright red-orange solution is formed, with an electronic spectrum very similar to those of $[Mo_2O_2(SAr)_6(OR')]^-$. Reaction is incomplete if the Fe:Mo ratio is less than 0.5. The red-orange solution is unstable and slowly turns yellow-brown, precipitating an insoluble brown solid. Rapid evaporation of the freshly prepared solution (Ar = Ph) followed by extraction with dry diethyl ether allows isolation of an orange powder which, on the basis of microanalysis and physical characterization (see Experimental Section), is probably $(Et_4N)[Mo_2O_2(SPh)_6Cl]$ contaminated with a little $FeCl_2$ or $FeCl_3$. Diphenyl disulfide was recovered from the ether extract. Equation 4 is a possible interpretation of these observations,

$$2[MoO(SAr)_4]^- + FeCl_3 \rightarrow [Mo_2O_2(SAr)_6Cl]^- + FeCl_2 + {}^1/_2ArSSAr + ArS^- \quad (4)$$

i.e., $FeCl_3$ oxidizes 1 mol of ArS^- and its removal promotes association of the $\{MoO(SAr)_3\}$ species with $[MoO(SAr)_4]^-$.

If extraction with alcohols R'OH (R' = Me, Et, *i*-Pr) is substituted for extraction with ether, the salts $B[Mo_2O_2(SAr)_6(OR')]$ can be isolated in good yields. If R'_2NH (R' = Et, *n*-Pr) is added to the acetonitrile solution before evaporation and extraction with ether, the salts $B[Mo_2O_2(SAr)_6(NR'_2)]$ (Table I) are obtained.

Physical Characterization of the Compounds. Infrared, magnetic moment, and conductance data are shown in Table IX. Frequencies most probably associated with the MoO groups of the three 2-oxoethanethiolate complexes occur (in the solid state) as two or three bands in the range 918–951 cm^{-1}. The symmetric and antisymmetric stretching frequencies expected[2] for coupled Mo–O oscillators may be present in these multiplets. Strong absorptions are observed in the ranges 908–915 and 931–943 cm^{-1} for the salts $B[Mo_2O_2(SCH_2Ph)_7]$ and $B[Mo_2O_2(SAr)_6Z]$, respectively. Shoulders at 923–932 and 927–933 cm^{-1}, respectively, may also indicate the presence of both the symmetric and antisymmetric modes.

Absorptions assigned[18-21] to the CO stretching frequency of bridging alkoxy groups occur in the range 1039–1055 cm^{-1} for the ^-OMe and ^-OEt complexes, and as multiple bands in the range 1023–1073 cm^{-1} for the $^-OCH_2CH_2S^-$ compounds. Absorptions in the 890–895-cm^{-1} region for the ^-OEt derivatives can be correlated[19,21] with the presence of bridging ethoxy groups.

Conductance measurements in the concentration range 10^{-2}–10^{-4} M in acetonitrile produce linear Onsager plots[22] (Λ_e vs. $c^{1/2}$), and the derived parameters Λ_o and A are included in Table IX. The slopes A (222–520) can be compared with those previously obtained[7] for the salts B^+X^- (X = halide) (217–543) and $B^+[MoO(SAr)_4]^-$ (273–530) and for a selection[23] (metal dithiolene complexes) of 1:1 (340–460) and 2:1 (660–900) conductors in acetonitrile. It is apparent that the compounds $B[Mo_2O_2(SR)_6Z]$, $(Et_4N)[Mo_2O_2(SCH_2CH_2O)_2Cl_3]$, and $(Et_4N)[Mo_2O_2(SCH_2CH_2O)_3Cl]$ are 1:1 conductors in acetonitrile and consequently contain binuclear monoanions.

Analytically pure samples of $B[Mo_2O_2(SAr)_6Z]$ in acetonitrile solution can show ESR signals whose parameters are very similar to those obtained[7] for the corresponding paramagnetic (μ_{eff} about 1.7 μ_B) mononuclear salts $B[MoO(SAr)_4]$. Careful observation reveals no half-field lines characteristic of spin triplet binuclear species. Successive recrystallizations of the salts $(Et_4N)[Mo_2O_2(SAr)_6(OMe)]$ (Ar = Ph, *p*-tolyl) and $(Et_3NH)[Mo_2O_2(SPh)_6(OMe)]\cdot MeOH$ eventually eliminate the signal and cause a concomitant decrease in the

Table IX. Infrared, Magnetic, and Conductance Data

compound			IR, cm^{-1}		magnetic moment,[b]	conductance parameters[c]	
			ν(Mo-O)[a]	ν(C-O)[a]	μ_B	Λ_0	A
$B^+[Mo_2O_2(SR)_6Z]^-$ B	R	Z					
Et_4N	CH_2Ph	SCH_2Ph	908		0.38	119	336
Ph_4As	CH_2Ph	SCH_2Ph	915		0.97	97	520
Ph_3MeP	CH_2Ph	SCH_2Ph	913		0.40		
Et_3NH[d]	Ph	OMe	940	1049	0.29	119	243
Et_4N	Ph	OMe	936	1048	0.32	125	228
Ph_3PNPPh_3	Ph	OMe	941	1040	0.42		
Et_4N	Ph	OEt	939	1039	0.63	134	236
Et_4N	Ph	O-*i*-Pr	931				
Et_4N	*p*-MeC_6H_4	OMe	940	1048	0.39	120	245
Ph_3MeP	*p*-MeC_6H_4	OMe	938	1055		108	429
Et_4N	*p*-MeC_6H_4	OEt	942	1039	0.64	125	351
Et_4N	Ph	NEt_2	937		0.44	139	222
Et_4N	*p*-MeC_6H_4	NEt_2	943				
Et_4N	Ph	N-*n*-Pr_2	937		0.38		
$(Et_4N)[Mo_2O_2(SCH_2CH_2O)_2Cl_3]$			951	1023	0.25	160	372
			942	1065			
			935				
$(Et_4N)[Mo_2O_2(SCH_2CH_2O)_3Cl]$			938	1031		130	285
			929 sh	1045			
				1073			
$(Pr_3NH)[Mo_2O_2(SCH_2CH_2O)_3(SCH_2CH_2OH)]$			944	1034			
			939	1050			
			918 sh	1064			

[a] Nujol mulls. [b] Per mole of Mo, in solid state at room temperature. [c] Concentration range 10^{-4}–10^{-2} M in acetonitrile at 25 °C. [d] Contains one molecule of MeOH of crystallization.

observed magnetic moment. For example, the magnetic moment of $(Et_4N)[Mo_2O_2(SPh)_6(OMe)]$ dropped from 0.53 to 0.32 μ_B over two recrystallizations. Consequently, the magnetic moments listed for these three compounds in Table IX can be regarded as unaffected by contaminating mononuclear Mo(V) species, whereas those for the other arylthiolate complexes may be slightly high (0.1–0.2 μ_B). No ESR signals were observed for the $PhCH_2S$ complexes or for $(Et_4N)[Mo_2O_2(SCH_2CH_2O)_2Cl_3]$ and $(Et_4N)[Mo_2O_2(SCH_2CH_2O)_3Cl]$, which is consistent with the apparent instability (or nonexistence) of corresponding mononuclear species. Solid $(Ph_4As)[Mo_2O_2(SCH_2Ph)_7]$ exhibits a higher magnetic moment than observed for the other salts, and the recorded value is essentially unchanged from sample to sample and after successive recrystallizations. The magnetic moments are field independent and characteristic of antiferromagnetically coupled Mo(V) species. Cations are known to influence the extent of such coupling in binuclear species,[24] and similar effects may account for the high magnetic moment of $(Ph_4As)[Mo_2O_2(SCH_2Ph)_7]$.

The 100-MHz ^1H NMR spectrum of $(Et_4N)[Mo_2O_2(SCH_2CH_2O)_2Cl_3]$ in CD_3CN solution shows the Et_4N^+ resonances centered at δ 1.20 and 3.15 (Me_4Si), but the 2-oxoethanethiolate resonances are poorly resolved at δ 3.7–4.55 (ca. 6 H) and δ 5.65–5.80 (ca. 2 H). The ^1H NMR spectra of the $B[Mo_2O_2(SR)_6Z]$ species were broad and poorly resolved.

Significantly absent from the electronic spectra of these complexes (Figure 2, Table VIII) is the intense (ϵ ca. 6000 cm^{-1} M^{-1}) absorption at 600 nm characteristic[7] of the mononuclear $[MoO(SAr)_4]^-$ complexes.

Description of the Structures. Comparable views (from the side opposite the oxo atoms) of the three homologous complexes containing the $^-OCH_2CH_2S^-$ ligand are shown in Figures 3, 4, and 5. Figure 6 shows the interion hydrogen bonds in $(Pr_3NH)[Mo_2O_2(SCH_2CH_2O)_3(SCH_2CH_2OH)]$.

The common $Mo_2O_2(SCH_2CH_2O)_2$ core consists of two MoO groups bridged by three atoms, namely, the oxygen (OS1) and sulfur (S1) atoms of one $^-OCH_2CH_2S^-$ ligand and the oxygen atom (OS2) of a second $^-OCH_2CH_2S^-$ ligand which also chelates Mo2 such that the thiolate group (S2) is terminally bound. The remaining three coordination positions (all terminal) of the core are structurally equivalent in the three complexes and are filled by 3 Cl^-, $^-OCH_2CH_2S^-$ plus Cl^-, or $^-OCH_2CH_2S^-$ plus $^-SCH_2CH_2OH$. The molybdenum atoms have similar coordination stereochemistry but different donor atoms in each of the three structures.

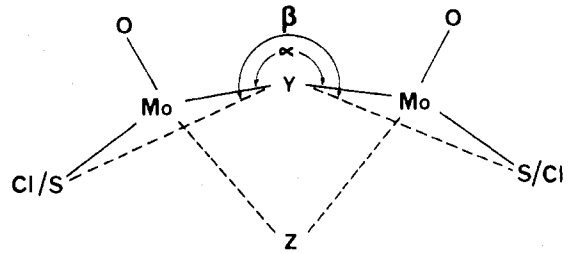

Figure 7. Definition of dihedral angles for binuclear (OMo)YY'Z(MoO) complexes.

This structure type could be regarded as two molybdenum coordination octahedra sharing a face, but the coordination stereochemistry of each molybdenum atom is better interpreted as square pyramidal with a sixth more distant ligand (ethanolate OS1) approximately trans to the apical Mo=O function. Table X sets out the displacements of pertinent atoms from the approximate planes which occur in the complexes, and Table XI contains significant dihedral angles. The molybdenum equatorial coordination planes are well developed; values for the displacement of each molybdenum atom from the equatorial plane toward the apical oxygen atom range from 0.30 to 0.38 Å. Values for the elongation of the sixth coordination bond length (i.e., [d(Mo1–OS1) – d(Mo1–OS2)] and [d(Mo2–OS1) – d(Mo2–OS2)]) range from 0.11 to 0.21 Å, with a mean of 0.15 Å. When the complexes are regarded as two square-pyramidal coordination polyhedra sharing an edge, there are two dihedral angles of interest, α and β, as defined in Figure 7; the mean values are α = 195° and β = 224°.

Table X. Atom Displacements (Å) from Molecular Planes

	Mo1 equator			Mo2 equator			bridging chelate ligand			Mo_2O_2		
	I	II	III	I	II	III	I	II	III	I	II	III
Mo1	(−0.30)[a]	(0.34)[a]	(0.35)[a]							+0.02	+0.03	+0.02
Mo2				(−0.35)	(0.33)	(0.38)				−0.02	−0.03	−0.02
S1	+0.01	−0.02	0.00	−0.02	+0.02	+0.01	0.00	0.00	0.00			
OS2	−0.01	+0.03	0.00	+0.03	−0.02	−0.01						
S2				−0.03	+0.02	+0.01						
Cl1/S4				+0.02	−0.02	−0.01						
Cl2/S3	−0.01	+0.03	0.00									
Cl3/OS3	+0.02	−0.03	0.00									
O1	(−1.95)	(2.00)	(2.03)							−0.01	−0.02	−0.01
O2				(−2.00)	(1.99)	(2.05)				+0.01	+0.02	+0.01
OS1							0.00	+0.01	0.00	(0.33)	(−0.32)	(0.25)
CS11							0.00	+0.01	+0.01			
CS12							0.00	−0.01	−0.01			

[a] Values in parentheses were excluded from least-squares plane calculations.

Table XI. Angles Involving Molecular Planes

angle	I	II	III
α (see Figure 7) planes: (Mo1, S1, OS2)-(Mo2, S1, OS)	196.6	196.4	191.5
β (see Figure 7) planes: (S1, OS2, Cl2/S3, Cl3/OS3)-(S1, OS2, S2, Cl1/S4)	224.0	224.3	222.6
planes: (Mo1, Mo2, O1, O2)-(S1, OS1, CS11, CS12)	91.3	89.4	89.4
(vector Mo1–OS1)–(normal to plane S1, OS2, Cl2/S3, Cl3/OS3)	17.4	17.7	17.4
(vector Mo2–OS1)–(normal to plane S1, OS2, S2, Cl1/S4)	17.9	17.2	18.3
torsional angle: S2–CS21–CS22–OS2	50.6 (5)	50 (1)	51.6 (6)
torsional angle: S3–CS31–CS32–OS3		34 (3)	50.0 (8)

The doubly bridging $^-OCH_2CH_2S^-$ ligand, 1, is effectively planar (excluding hydrogen atoms), whereas the chelate rings of $^-OCH_2CH_2S^-$, ligands 2 and 3, possess a skew conformation, with the S–C–C–O torsional angles only slightly less than the value (58.3°) in uncoordinated 2-hydroxyethanethiol.[25]

Bond distances and angles, given in Tables VI and VII, are not abnormal. There is no significant difference in length between the terminal Mo–S (mean 2.384 Å) and Mo–Cl (mean 2.386 Å) bonds, although the Mo–S distances show greater variation. The terminal Mo–S bond lengths observed here are slightly less than other comparable values for OMo^V–thiolate coordination, namely, 2.41 ± 0.01 Å[26] in $[MoO(SPh)_4]^-$,[9] 2.45 ± 0.03 Å[26] in $[Mo_2O_4(SPh)_4]^{2-}$,[8] and 2.41 ± 0.01 Å[26] in the syn and anti isomers of $[Mo_2S_4(SCH_2CH_2CH_2S)_2]^{2-}$.[27] Terminal OMo^V–Cl distances in other structures range from 2.33 Å in $[OMoCl_4]^-$[28] to 2.42 Å in $[Mo_2O_4Cl_4]^{2-}$.[29] The mean length for the Mo-bridging thiolate (S1) bond is 2.481 Å, an elongation of 0.10 Å over the comparable Mo–terminal thiolate bond length. This elongation is of similar magnitude to that measured in complexes of other metals containing both terminal and bridging thiolate ligands.[30,31] The six Mo–OS1 distances are quite variable, which is consistent with the weaker bonding ascribed to this interaction.

The uncoordinated hydroxy function of ligand 4 in $(Pr_3NH)[Mo_2O_2(SCH_2CH_2O)_3(SCH_2CH_2OH)]$ is involved in two hydrogen bonds (see Figure 6), one of which (OS4—HOS4···OS3′) links to coordinated alkoxide oxygen in another complex anion, while the other (OS4···HN—N) links with the tripropylammonium cation. The overall distances are OS4···OS3′ = 2.702 (6) Å and OS4···N = 2.748 (6) Å.

Discussion

A significant aspect of the structures of the three 2-oxoethanethiolate complexes is the triple bridge between the two MoO groups and the geometry of its construction from two $^-OCH_2CH_2S^-$ ligands. Although we have also obtained and characterized complexes in which the triple bridge is constructed from one $^-OCH_2CH_2S^-$ ligand and one oxide ion, O^{2-}, it appears that the new $\{Mo_2O_2(SCH_2CH_2O)_2\}$ core is a prevalent feature of the $OMo(V)/^-OCH_2CH_2S^-$ system.

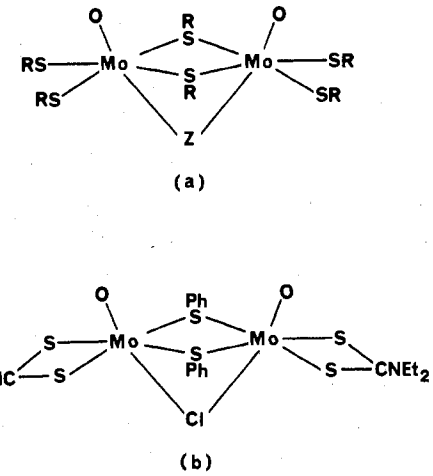

Figure 8.

So far all crystals of the complexes $B[Mo_2O_2(SR)_6Z]$ have proven to be unsuitable for X-ray structure determination. However, the presence of a triply bridged structure, Figure 8a, is strongly suggested by the available evidence: (i) The physical data indicate the presence of a binuclear monoanion $[Mo_2O_2(SR)_6Z]^-$, containing at least one terminal oxo–molybdenum bond, and, for Z = OR′, a bridging alkoxy ligand. (ii) The physical properties of $B[Mo_2O_2(SR)_6Z]$ and the three structurally characterized $^-OCH_2CH_2S^-$ complexes are very similar (Tables VIII, IX). In both sets of compounds the seven variable ligands are thiolate, alkoxide, or chloride groups, all analogous monoanions. (iii) The closely related species $[Mo_2O_2(SPh)_2Cl(S_2CNEt_2)_2]^+$ (Figure 8b, Table XII) contains[5] equivalent benzenethiolate bridges and Cl as the unique bridging ligand Z; the dithiocarbamate ligands are terminal.

Consequently, all of the $[Mo_2O_2(SR)_6Z]^-$ anions are assigned the triple-bridged structure of Figure 8a.

Table XII is a comparative collection of the significant details for structurally characterized instances of the triply bridged bis(oxomolybdenum(V)) unit of Figure 1d. The bridging groups are thiolate, alkoxide, chloride, oxide, or sulfide. Details are available for one other structure containing $^-OCH_2CH_2S^-$ as part of a triple bridge, namely, $[Mo_2O_3(SCH_2CH_2O)(ox)_2]$ (oxH = 8-hydroxyquinoline). Despite the substantial chemical differences between this complex and

Table XII. Structural Features of Triply Bridged Oxomolybdenum(V) Complexes

complex	Y[a]	Y′	Z	Mo–Mo, Å	Mo[b] displacement, Å	α,[c] deg	Mo–Z–Mo, deg	Mo–Y–Mo, deg	Mo–Y′–Mo, deg	mean Y–Mo–Y′, deg	ref
$[Mo_2O_2(SCH_2CH_2O)_2Cl_3]^-$	RS^-	RO^-	RO^-	2.73	0.30, 0.35	196.6	77.6	66.7	85.2	103.0	this work
$[Mo_2O_2(SCH_2CH_2O)_3Cl]^-$	RS^-	RO^-	RO^-	2.73	0.33, 0.34	196.4	77.7	66.8	84.9	103.2	this work
$[Mo_2O_2(SCH_2CH_2O)_3(SCH_2CH_2OH)]^-$	RS^-	RO^-	RO^-	2.74	0.38, 0.35	191.5	77.2	67.0	83.6	104.2	this work
$[Mo_2O_3(SCH_2CH_2O)(ox)_2]$	RS^-	O^{2-}	RO^-	2.63	0.39	195.9	73.8	63.9	85.5	104.5	4
$[Mo_2O_2S(SCH_2CH_2O)(S_2CNEt_2)_2]$	RS^-	S^{2-}	RO^-	2.73	0.39	195.4	76.5	66.4	71.4	110.4	14
$[Mo_2O_3(SPh)_2(S_2CNEt_2)_2]$[d]	ArS^-	O^{2-}	ArS^-	2.68	0.39	178.0	59.9	65.0	83.7	105.6	6
				2.67			59.7	64.9	80.2	107.5	
$[Mo_2O_2(SPh)_2Cl(S_2CNEt_2)_2]^+$	ArS^-	ArS^-	Cl^-	2.82	0.40	182.3	65.4	70.0	70.2	109.9	5

[a] See Figure 1d. [b] Displacement of the Mo atom from the ligand equatorial plane. [c] Dihedral angle between the two MoYY′ planes; see Figure 8. [d] Two crystallographically independent molecules exist in the structure.

those reported in this paper, including the fact that the third bridging atom is oxide rather than alkoxide, the geometry of the bridge is essentially the same in all four structures. The geometrical consequence of alkoxide vs. oxide as the bridging ligand Y′ is an increase of 0.07 Å in Mo–O distance in the former case and a concomitant increase of 0.10 Å in the Mo–Mo distance.

In turning to general consideration of the geometry of triply bridged MoO complexes (Figure 1d), the geometry of doubly bridged MoO complexes is first reviewed. Factors which contribute to the observed geometry of compounds containing the $[Mo_2O_2X_2]^{2+}$ (X = O, S) structural unit in the syn isomer (Figure 1c) can be summarized:[2,3] (a) Tetragonal distortion: the strong MoO triple bond causes each Mo to lie significantly out of the equatorial coordination plane toward the oxo group, and the bond *trans* to the *oxo* group is elongated or absent. (b) Mo–Mo bonding: the short Mo–Mo distances, the observed Mo–X–Mo and X–Mo–X angles, and the low magnetic moments are consistent with direct intermetal interactions. (c) Nonbonded repulsions: bond angles involving first the terminal oxo groups (bent back away from each other) and second the bridging X groups indicate the influence of nonbonded interatomic repulsions. A noteworthy feature in these doubly bridged structures is a dihedral angle α in the range 140–160°.

Factors (a)–(c) are also pertinent to the structures of the triply bridged complexes. The existence of seven structure determinations (Table XII) for triply bridged species allows some additional observations to be made: (d) Substitution of one or both of the bridging monoatomic *di*anionic ligands X^{2-} in $[Mo_2O_2X_2]^{2+}$ by a *mono*anionic ligand leads to a preference for the triply bridged structure. Apparently two dianions X^{2-} can introduce sufficient electron density into the bridge region that a third bridging ligand is unnecessary.[32] (e) The formation of the triple bridge leads to an increase in the dihedral angle α to 180–196° (Table XII), which is essential for reasonable Mo–Z–Mo angles. (f) The steric influence of a doubly bridging $^-OCH_2CH_2S^-$ ligand occupying the Y and Z positions is seen, in dihedral angles α at the top of the range, leading to larger (and presumably more favorable) Mo–Z–Mo bond angles. Essentially the same bridge geometry is maintained despite variation of the Y′ ligand through OR^-, O^{2-}, or S^{2-} and considerable variation in the chemical nature of the terminal ligands. (g) All triply bridged species characterized structurally to date involve at least one thiolate ligand in the bridge.[35] If a single dianionic ligand X^{2-} is present it occupies a Y, not Z, position. The Z position can be occupied by Cl^-, RO^-, R_2N^-, or RS^- ligands. However, ArS^- appears not to favor the Z position, perhaps for steric reasons. Thus, $[Mo_2O_3(SPh)_2(S_2CNEt_2)_2]$ is very reactive,[5] and species $[Mo_2O_2(SAr)_7]^-$ could not be isolated in the present work. The mononuclear species $[MoO(SAr)_4]^-$ are stable until a source of ligand suitable for the Z position (Cl, RO, R_2N) is made available. Indeed, addition of 1 molar equiv of $PhCH_2SH$ to a solution of $[MoO(SAr)_4]^-$ induces dimerization, revealed by a change of color from deep blue to orange-red.

Our results are further indication of the prevalence of the triple bridge as a structural feature of oxomolybdenum(V) chemistry. In particular, (i) synthesis of mononuclear oxomolybdenum(V) complexes will need careful ligand design to circumvent the formation of triply bridged binuclear species, and (ii) it is becoming evident that the $^-OCH_2CH_2S^-$ chelate as an asymmetric part of a triple bridge between two OMo groups is a significant structural component for solutions containing Mo(V) and 2-hydroxyethanethiol. $(Et_4N)[Mo_2O_2(SCH_2CH_2O)_2Cl_3]$ is a valuable precursor for the synthesis and systematic study of complexes in this new class.[36]

Acknowledgment. This work is supported by the Australian Research Grants Committee. I.W.B. acknowledges the receipt of a Commonwealth Postgraduate Scholarship. We thank D. C. Craig for assistance with the collection of diffraction data.

Registry No. I, 69532-63-4; II, 69532-65-6; III, 69532-67-8; $Et_4N[Mo_2O_2(SCH_2Ph)_7]$, 69532-57-6; $Ph_4As[Mo_2O_2(SCH_2Ph)_7]$, 69609-02-5; $Et_4N[Mo_2O_2(S(CH_2)_3S)_3OMe]$, 69576-59-6; $Ph_4As[Mo_2O_2(S(CH_2)_2S)_3OMe]$, 69532-59-8; $Et_3NH[Mo_2O_2(SPh)_6OMe]$, 69532-61-2; $Et_4N[Mo_2O_2(SPh)_6OMe]$, 69609-04-7; $Ph_3PNPPh_3[Mo_2O_2(SPh)_6OMe]$, 69609-05-8; $Et_4N[Mo_2O_2(SPh)_6OEt]$, 69532-69-0; $Et_4N[Mo_2O_2(SPh)_6O\text{-}i\text{-}Pr]$, 69532-71-4; $Et_4N[Mo_2O_2(S\text{-}p\text{-}MeC_6H_4)_6OMe]$, 69532-73-6; $Ph_3MeP[Mo_2O_2(S\text{-}p\text{-}MeC_6H_4)_6OMe]$, 69609-06-9; $Et_4N[Mo_2O_2(S\text{-}p\text{-}MeC_6H_4)_6OEt]$, 69532-75-8; $Et_4N[Mo_2O_2(SPh)_6NEt_2]$, 69532-77-0; $Et_4N[Mo_2O_2(S\text{-}p\text{-}MeC_6H_4)_6NEt_2]$, 69532-79-2; $Et_4N[Mo_2O_2(SPh)_6N\text{-}n\text{-}Pr_2]$, 69532-81-6; $Ph_3MeP[Mo_2O_2(SCH_2Ph)_7]$, 69609-07-0; $Et_4N[Mo_2O_2(SPh)_6Cl]$, 69532-83-8; $Et_4N[MoOCl_4(OH)_2]$, 57127-49-8; $MoOCl_3(THF)_2$, 20529-42-4; $Et_4N[MoO(SPh)_4]$, 65892-35-5; $(Et_4N)_2[MoO_2(NCS)_4]$, 58616-90-3.

Supplementary Material Available: Listings of analytical data (Table S1), F_o and F_c (Tables S2, S3, S4) and atomic thermal parameters (Tables S5, S6, S7) for the three structures, powder diffraction data (Table S8), and cation distances (Table S9) (45 pages). Ordering information is given on any current masthead page.

References and Notes

(1) (a) La Trobe University. (b) University of New South Wales.
(2) E. I. Stiefel, *Prog. Inorg. Chem.*, **22**, 1 (1977).
(3) B. Spivack and Z. Dori, *Coord. Chem. Rev.*, **17**, 99 (1975).
(4) J. I. Gelder, J. H. Enemark, G. Wolterman, D. A. Boston, and G. P. Haight, *J. Am. Chem. Soc.*, **97**, 1616 (1975).
(5) G. Bunzey, J. H. Enemark, J. I. Gelder, K. Yamanouchi, and W. E. Newton, *J. Less-Common. Met.*, **54**, 101 (1977).
(6) K. Yamanouchi, J. H. Enemark, J. W. McDonald, and W. E. Newton, *J. Am. Chem. Soc.*, **99**, 3529 (1977).
(7) I. W. Boyd, I. G. Dance, K. S. Murray, and A. G. Wedd, *Aust. J. Chem.*, **31**, 279 (1978).
(8) I. G. Dance, A. G. Wedd, and I. W. Boyd, *Aust. J. Chem.*, **31**, 519 (1978).
(9) J. R. Bradbury, M. F. Mackay, and A. G. Wedd, *Aust. J. Chem.*, **31**, 2423 (1978).
(10) K. Garbett, R. D. Gillard, P. F. Knowles, and J. E. Stangroom, *Nature (London)*, **215**, 824 (1967).
(11) J. L. Johnson and K. V. Rajagopalan, *J. Biol. Chem.*, **252**, 2017 (1977).
(12) A. Kay and P. C. H. Mitchell, *J. Chem. Soc. A*, 2421 (1970).
(13) W. E. Newton, G. J. J. Chen, and J. W. McDonald, *J. Am. Chem. Soc.*, **98**, 5387 (1976).
(14) J. T. Huneke, K. Yamanouchi, and J. H. Enemark, Abstracts, 175th National Meeting of the American Chemical Society, Anaheim, Calif., March 1978, No. INOR-18; *Inorg. Chem.*, **17**, 3695 (1978).

(15) B. J. Brisdon and D. A. Edwards, *Inorg. Nucl. Chem. Lett.*, **10**, 301 (1974).
(16) "International Tables for X-Ray Crystallography", Vol. IV, Kynoch Press, Birmingham, England, 1974, Tables 2.2A and 2.3.1.
(17) A. C. Larson in "Crystallographic Computing", F. R. Ahmed, Ed., Munksgaard, Copenhagen, 1970, p 291.
(18) T. Inazu, H. Okawa, and T. Yoshino, *Bull. Chem. Soc. Jpn.*, **42**, 2291 (1969).
(19) K. Kasuga, T. Hon, and Y. Yamamoto, *Bull. Chem. Soc. Jpn.*, **47**, 1026 (1974).
(20) J. A. Bertrand and R. I. Kaplan, *Inorg. Chem.*, **4**, 1657 (1965).
(21) C. H. S. Wu, G. R. Rossman, H. B. Gray, G. S. Hammond, and H. S. Schugar, *Inorg. Chem.*, **11**, 990 (1972).
(22) W. S. Geary, *Coord. Chem. Rev.*, 7, 781 (1971).
(23) J. F. Coetzee and G. R. Cunningham, *J. Am. Chem. Soc.*, **87**, 2529 (1965); M. S. Elder, G. M. Prinz, P. Thornton, and D. H. Busch, *Inorg. Chem.*, **7**, 2426 (1968); A. Davison, D. V. Howe, and E. J. Shawl, *ibid.*, **6**, 458 (1967); F. A. Cotton, W. R. Robinson, R. A. Walton, and R. Whyman, *ibid.*, **6**, 929 (1967).
(24) P. W. Smith and A. G. Wedd, *J. Chem. Soc. A*, 2447 (1970); I. E. Grey and P. W. Smith, *Aust. J. Chem.*, **22**, 121 (1969).
(25) E. M. Sung and M. D. Harmony, *J. Am. Chem. Soc.*, **99**, 5603 (1977).
(26) The uncertainties quoted as ± are estimated standard deviations of the sample of values measured for each structure.
(27) G. Bunzey and J. H. Enemark, *Inorg. Chem.*, **17**, 682 (1978).
(28) C. D. Garner, L. H. Hill, F. E. Mabbs, D. L. McFadden, and A. T. McPhail, *J. Chem. Soc., Dalton Trans.*, 853 (1977).
(29) R. Mattes, D. Altmeppen, and M. Fetzer, *Z. Naturforsch.*, **316**, 1356 (1976).
(30) I. G. Dance and J. C. Calabrese, *J. Chem. Soc., Chem. Commun.*, 762 (1975).
(31) I. G. Dance, *J. Chem. Soc., Chem. Commun.*, 103 (1976); *Aust. J. Chem.*, in press.
(32) The anion $[Mo_2O_4(NCS)_4(CH_3CO_2)]^{3-}$ contains[33] an Mo_2O_4 unit supplemented by a bridging bidentate acetate ligand, whose bite allows it to supply a ligand atom at positions trans to both terminal oxo groups, completing six-coordination around each molybdenum. This and similar species[34] are closely related to the $Mo_2O_2X_2$-based structures (Figure 1c) and not relevant to the triply bridged species discussed here.
(33) T. Glowiak, M. Sabat, H. Sabat, and M. F. Rudolf, *J. Chem. Soc., Chem. Commun.*, 712 (1975).
(34) B. Jezowska-Trzebiatowska, M. F. Rudolf, L. Natkamic, and H. Sabat, *Inorg. Chem.*, **13**, 617 (1974); T. Glowiak, M. F. Rudolf, M. Sabat, and B. Jezowska-Trzebiatowska, *J. Less-Common Met.*, **54**, 35 (1977).
(35) However, the compound $[Mo_2O_3Cl_2L_2]$ (LH = 8-aminoquinoline) appears to contain a triple bridge consisting of an oxo and two (inequivalent) NH groups from the amido functions of the quinolate ligand: I. W. Boyd and A. G. Wedd, unpublished results.
(36) I. G. Dance, unpublished results.

Contribution from the School of Chemical Sciences, University of Illinois, Urbana, Illinois 61801

Complexes as Ligands. 2. Structural, Spectral, and Magnetic Properties of the Bimetallomer Formed from *N,N'*-Ethylenebis(salicylideniminato)copper(II) and Bis(hexafluoroacetylacetonato)copper(II)

KENNETH A. LESLIE, RUSSELL S. DRAGO,* GALEN D. STUCKY,* DAVID J. KITKO, and JOHN A. BREESE

Received October 6, 1978

As a continuation of our studies of complexes as ligands, we have investigated the bimetallomer Cu(salen)Cu(hfac)$_2$, which is the adduct formed by the reaction of the Lewis base *N,N'*-ethylenebis(salicylideniminato)copper(II) with the Lewis acid bis(hexafluoroacetylacetonato)copper(II). Since this bimetallomer contains two different copper(II) environments (six-coordinate and four-coordinate), magnetic susceptibility and EPR spectral studies were undertaken in order to characterize the system. Variable-temperature magnetic susceptibility measurements indicate an antiferromagnetic exchange interaction with a coupling constant, J, between the copper(II) centers of -20.4 cm^{-1}. In order to explain the relatively small value of J when compared to that of symmetric copper(II) bimetallomers, a single-crystal X-ray diffraction study was carried out. The compound crystallizes in the triclinic space group $P\bar{1}$ with four molecules in the unit cell. The reduced cell parameters are a = 17.03 (4) Å, b = 19.11 (4) Å, c = 9.89 (2) Å, α = 96.58 (11)°, β = 100.10 (16)°, and γ = 107.70 (13)°. The structure was refined by full-matrix least-squares methods to a weighted R factor of 0.074 for data with $F_o \geq 3\sigma_F$. The structural results indicate that the reduced value of J is due to the low symmetry of the bridge area which allows for only one phenolic oxygen to participate in the superexchange pathway.

Introduction

An earlier X-ray crystallographic investigation indicated[1] that the complexes Cu^{II}salen and $Co^{II}(hfac)_2$ reacted to form a bimetallomer in which the oxygen donor atom of salen was simultaneously coordinated to copper and cobalt. It was also shown that the following reaction, leading to this product, was very rapid in dilute dichloromethane solution:

$$Co(salen) + Cu(hfac)_2 \rightarrow Cu(salen)Co(hfac)_2$$

The rapid metal swapping of a tetradentate chelate in CH_2Cl_2 was very surprising, and a kinetic study was undertaken to ascertain the mechanism.[2]

In the course of these studies, the complex Cu(salen)Cu(hfac)$_2$ was prepared. Since relatively few[3,4] copper(II) bimetallomers have been investigated in which the environment around the interacting coppers is different, magnetic investigations were undertaken. The difference in the results obtained for the complex from those expected[5,6] from theory and experiment for a symmetric bimetallomer (with a bridge angle corresponding to that found in the copper–cobalt adduct) led us to pursue a full structural characterization of the Cu(salen)Cu(hfac)$_2$ complex.

Experimental Section

Cu(salen)Cu(hfac)$_2$ was prepared as previously reported.[2] Anal. Calcd for $Cu_2C_{26}H_{16}N_2O_6F_{12}$: Cu, 15.74; C, 38.67; H, 2.00; N, 3.47; F, 28.23. Found: Cu, 15.82; C, 39.54; H, 2.00; N, 3.44; F, 28.22.

Ni(salen)Zn(hfac)$_2$ was prepared by the procedure described for Cu(salen)Co(hfac)$_2$.[1] Ni(salen) (0.98 g, 3 mmol) and Zn(hfac)$_2$·2H$_2$O (1.55 g, 3 mmol) were employed as starting materials, having been prepared from nickel acetate and zinc acetate, respectively; yield 2.0 g (79%). Anal. Calcd for $ZnNiC_{26}H_{16}N_2O_6F_{12}$: Zn, 8.13; Ni, 7.30; C, 38.82; H, 2.00; N, 3.48. Found: Zn, 8.05; Ni, 7.23; C, 38.45; H, 2.01; N, 3.41.

Physical Measurements. Variable-temperature (4.2–270 K) magnetic susceptibility measurements were carried out with a Princeton Applied Research Model 150A vibrating-sample magnetometer calibrated with $CuSO_4·5H_2O$.[7] All molar susceptibilities were corrected for diamagnetic contributions by using Pascal's constants.[8] A least-squares fitting of the data was carried out with the function minimization program STEPT.[9]

Electron spin resonance spectra were collected on a Varian Model E-9 spectrometer operating at ca. 9.1 GHz (X-band) and equipped

0020-1669/79/1318-1885$01.00/0